Journal of Sound and Vibration (1998) **214**(4), 639–658
Article No. sv981616

IDENTIFICATION OF NON-LINEAR SYSTEMS USING MULTI-SCALE RIDGES AND SKELETONS OF THE WAVELET TRANSFORM

W. J. Staszewski

*Dynamics Research Group, Department of Mechanical Engineering, University of Sheffield, Mappin Street, Sheffield S*1 3*JD, England*

(*Received* 8 *September* 1997, *and in final form* 17 *February* 1998)

A new procedure of non-linear system identification is presented. The procedure employs the slowly-varying, time-dependent amplitude and phase functions of the impulse response of the system. These instantaneous characteristics are obtained from the ridges and skeletons of the wavelet transform. The ridge extraction procedure uses the modulus of the transform and involves a combinatorial optimization algorithm based on simulated annealing. The method is illustrated using two simple simulated examples. It is shown that the procedure can be used for multi-degree-of-freedom systems due to the frequency localization property of the continuous Grossman–Morlet wavelets.

1. INTRODUCTION

All physical and engineering systems exhibit in practice non-linear behaviour to some degree. Non-linearities may arise from structural, geometric and material properties or due to damage of the structure. Since non-linear systems can display complex phenomena which linear systems cannot, the distinction between linear and non-linear systems is an important problem. Classical linear methods applied to non-linear structures provide no means of describing this complex phenomena. This analysis may also result in inaccuracies which are too significant to be neglected. Many different procedures have been developed in structural dynamics to analyze non-linear systems. The most relevant methods that can be employed in dynamic testing are summarized in reference [1]. Some of these methods detect non-linearities, others can characterize the type of non-linearity and/or identify structural parameters. The object of identification is to obtain a mathematical model on the basis of measured data. If the data is in the time domain (acceleration, force), the identification is said to be in the time domain. If the measured data takes the form of the frequency response function (FRF) or spectra, the analysis is said to be in the frequency domain. Time and frequency analysis has been extended to the use of phase plane, time–frequency, time–scale approaches, multi-dimensional spectra and models.

The first step in system identification begins with the choice of the input excitation. Transient response is obtained when the system is excited by a signal of short duration. This analysis does not appear to be commonly used for non-linear system identification. However, it offers some important advantages. Transient response exhibits oscillations at the natural frequencies of the system with the amplitude dependent on the type of excitation. Different types of excitation can be used to obtain transient response; impulse excitation, for example, displays the decay nature of vibration. Impulse excitation is very covenient for a wide variety of applications, especially in laboratory conditions. Different

0022–460X/98/290639 + 20 $30.00/0

excitation levels can be reached with a single dynamic test. Transient response based procedures do not need any information about the input excitation and allow a direct non-parametric identification.

It is well known that many types of non-linearities display varying natures of restoring forces and natural frequencies of the system. The most successful approach to studying this varying nature of vibration is offered by the Hilbert transform. The method uses the instantaneous amplitude and frequency of the impulse response function in order to obtain the backbone curve and the instantaneous logarithmic decrement of the system. These characteristics give quantitative information about the non-linear behaviour. The method was developed in the 1980s [2, 3] and has received much attention since that time [4–9]. Despite its success, the Hilbert transform procedure is limited to some types of applications. The limitation of the method comes from the fact that the Hilbert transform based envelope and instantaneous frequency is valid only for asymptotic signals, i.e., signals which have slowly varying amplitudes compared with phase variations. Even if the asymptotic signals are used, the Hilbert transform method requires a signal filtration and differentiation procedure; the latter is not any easy task [10]. In order to avoid these drawbacks the Wigner–Ville distribution [11, 12] and Gabor transform [13] based procedures have been used to study the non-linear nature of instantaneous vibration characteristics. The techniques developed using the Hilbert transform and Wigner–Ville distribution give the most effective results for single-degree-of-freedom (SDOF) systems. Applications to multi-degree-of-freedom (MDOF) systems have proved difficult since the analysis requires bandpass filtration of the signal. This can produce complicated results, and even fail, if system modes are close in frequency.

Recent developments in the area of time–scale analysis open some possibilities in using the wavelet transform to study non-linear vibration. Unfortunately, non-linear system identification has not fully benefited from these developments. A few attempts [14–16] have been made to detect non-linearities from the amplitude and phase plots of the wavelet transform. Other applications involve: extraction of impulse response function [17–19], identification of damping [19, 20], time-dependent FRFs [16] and general system identification procedures based on wavelet localization and filtration properties [21–23]. There also exists a number of applications limited to fault detection procedures; those related to structural damage detection include references [24–26]. More recently, the procedure based on the impulse response function and the wavelet analysis has been proposed by the author [27, 28]. The method uses the wavelet transform ridges of the impulse response functions in order to obtain the backbone curve of the system. The ridge detection procedure was based on the phase of the transform. This could be ineffective in noisy situations. The method has been used for a SDOF system exhibiting a cubic stiffness non-linearity.

The aim of this paper is to present an identification procedure for MDOF non-linear systems. The procedure is based on ridges and skeletons of the wavelet transform. The ridge detection procedure uses the amplitude of the transform and involves combinatorial optimization. The paper comprises two major parts. The first part includes sections 2 and 3. Most of the material presented in these sections has been already reported. However, for the sake of completeness and better understanding of identification procedures it is necessary to bring some of these developments together. This is especially important for newcomers to wavelet analysis. Thus, the wavelet transform is briefly introduced in section 2. The ridges and skeletons of the wavelet transform are described in section 3. The algorithm of ridge extraction is given in the Appendix. Sections 4 and 5 form the new developments relating to the analysis of non-linear systems. The identification procedure based on the wavelet transform ridges is given in section 4. Examples of application to

simulated non-linear systems are presented in section 5. Finally, the paper is concluded in section 6.

2. CONTINUOUS WAVELET TRANSFORM

A linear transformation which decomposes a function in terms of a basis of elementary functions can be achieved by the Fourier transform. This decomposition does not give any local time information about the function due to the infinite nature of the trigonometric functions used in the analysis. One of the most rapidly evolving methods which provides for locality is the wavelet transform. This section briefly introduces the continuous wavelet transform. The reader is referred to references [29–31] for a historical perspective and more detailed mathematical theory or to references [32, 33] for vibration and signal processing applications.

2.1. DEFINITION

A wavelet $\psi(t)$ is a square integrable function which holds the following admissibility condition.

$$0 < C_\psi = \int_{-\infty}^{+\infty} \frac{|\Psi(f)|^2}{|f|}\,\mathrm{d}f < \infty, \tag{1}$$

where $\Psi(f)$ is the Fourier transform of $\psi(t)$. A whole family of equally shaped functions can be generated from this wavelet by shifts in time domain (b-translation) and scaling in the scale domain (a-dilation),

$$\psi_{a,b}(t) = \frac{1}{\sqrt{a}}\psi\left(\frac{t-b}{a}\right), \quad a > 0,\ b \in \Re. \tag{2}$$

The idea of the wavelet transform is to decompose a signal $x(t)$ into wavelet coefficients $(W_\psi x)(a, b)$ using the basis of wavelet functions $\psi_{a,b}(t)$. This can be expressed mathematically by the following equations,

$$(W_\psi x)(a, b) = \langle x, \psi_{a,b}\rangle = \int_{-\infty}^{+\infty} x(t)\psi^*_{(a,b)}(t)\,\mathrm{d}t, \tag{3}$$

where $\psi^*(\,\cdot\,)$ is the complex conjugate of $\psi(\,\cdot\,)$. The locality of the transform requires that $\psi(t)$ decays at infinity. Many applications impose additionally regularity and vanishing moments on wavelets. There are many functions used in practice as wavelets. In this paper, the Morlet wavelet [34] is used, being defined as,

$$\psi(t) = \mathrm{e}^{i2\pi f_0|t|}\,\mathrm{e}^{-|t|^2/2}. \tag{4}$$

Other wavelet functions used in pratice can be found in reference [30].

2.2. BASIC PROPERTIES

A number of interesting properties of the wavelet transform have been studied and well documented, e.g., reference [31]. A brief summary of the properties used throughout this paper and important for the analysis in sections 3 and 4, is given below.

One of the most important properties of the wavelet transform is its conservation of energy formula, which in fact is a reconstruction. The concentration of energy in the time–scale domain is discussed in more detail in the next section.

Since the wavelet transform is a linear representation of a signal, it follows that for given N functions x_i, and N complex values α_i ($i = 1,2, \ldots, N$),

$$\left(W_\psi \sum_{i=1}^{N} \alpha_i x_i\right)(a, b) = \sum_{i=1}^{N} \alpha_i (W_\psi x_i)(a, b). \tag{5}$$

This property is useful for the analysis of multi-component signals.

It is clear from the definition that the Fourier transform extracts periodic infinite waves from the analyzed function. In contrast, the wavelet transform analyzes a function only locally at windows defined by a wavelet function. The frequency localization is clearly seen when the wavelet transform is expressed in the frequency domain,

$$(W_\psi x(a, b) = \sqrt{a} \int_{-\infty}^{+\infty} X(f) \Psi^*_{a,b}(af)\, \mathrm{e}^{j2\pi fb}\, \mathrm{d}f, \tag{6}$$

where $\Psi^*(\cdot)$, is the complex conjugate of $\Psi(\cdot)$. This localization depends on the dilation parameter a. The local resolution of the wavelet transform in time and frequency is determined by the duration and bandwidth of analyzing functions given by reference [31],

$$\Delta t = a \Delta t_\psi, \qquad \Delta f = \frac{\Delta f_\psi}{a}, \tag{7}$$

where Δt_ψ and Δf_ψ are the duration and bandwidth of the basic wavelet function, respectively.

Although the wavelet transform is a time–scale decomposition, there is a relationship between scale parameter (dilation) and frequency [31]. For the Morlet wavelet given by equation (4), the relationship between the dilation parameter a_f and the signal frequency f_x at which the wavelet is focused, can be given as [35].

$$a_f = f_0 \frac{f_s}{f_w} \frac{1}{f_x}, \tag{8}$$

where f_s and f_w are the sampling frequencies of the signal and the analyzing wavelet, respectively. The frequency bandwidth of the wavelet function for the given dilation a_f can be expressed as,

$$\Delta f_x = \frac{1}{\pi a_f} \frac{f_s}{f_w}. \tag{9}$$

Equations (8) and (9) allow one to obtain a single element of the wavelet decomposition of the function for a given value of frequency (dilation) and frequency bandwidth.

3. RIDGES AND SKELETONS OF THE WAVELET TRANSFORM

For a physical interpretation, the square of the modulus of the wavelet transform can be interpreted as an energy density distribution over the (a, b) time–scale plane. The energy of a signal is mainly concentrated on the time–scale plane around the so called ridge of the wavelet transform. Following reference [36], the basic description of ridges and skeletons is presented in this section.

3.1. DEFINITIONS

Assuming that the signal and the wavelet are asymptotic, let us introduce some stationary points t_s of,

$$\overline{\phi}_{a,b}(t) = \phi_x(t) - \phi_\psi\left(\frac{t-b}{a}\right), \tag{10}$$

where ϕ_x and ϕ_ψ denote the instantaneous phases of the signal and the wavelet, respectively. Mathematically the ridge of the function is the curve $a = r(b)$, which consists of points (a, b) satisfying the condition $t_s(a, b) = b$ [36]. This means in practice that the wavelet transform gives the contribution of such stationary points to the scalar product between the signal and the wavelet in equation (3). The ridge of the wavelet transform is directly related to the instantaneous frequency of the signal. This property follows from the ridge definition [36]

$$r(b) = \frac{\dot{\phi}_\psi(0)}{\dot{\phi}_x(b)}. \tag{11}$$

The values of the wavelet transform restricted to its ridge form the skeleton of the wavelet transform, which can be represented as [36]

$$(W_\psi x)(r(b), t) = C(t)x_a(t), \tag{12}$$

where $C(t)$ is the correction function completely determined by the wavelet and the ridge and $x_a(t)$ is the analytic signal defined as

$$x_a(t) = x(t) + i\hat{x}(t), \tag{13}$$

where $\hat{x}(t)$ is the Hilbert transform of the $x(t)$ defined as

$$\hat{x}(t) = \frac{1}{\pi}\int_{-\infty}^{+\infty} x(\tau)\frac{1}{t-\tau}\,\mathrm{d}\tau. \tag{14}$$

This means in practice that the signal and its Hilbert transform are approximately given by the real and imaginary parts of the skeleton of the wavelet transform, respectively.

3.2. RIDGE EXTRACTION PROCEDURE

There exist different algorithms for the ridge extraction. The most usual one uses the local maxima of the amplitude of the transform. However, this algorithm gives exact values only for linear ridges. The better way of extraction can be obtained from the phase function. This algorithm was proposed by Tchamitchian and Torresani [36]. It uses the following properties of the ridge [36],

$$\frac{\partial\Omega(a, b)}{\partial a} = 0, \qquad \left[\frac{\mathrm{d}\Omega(a, b)}{\mathrm{d}b}\right]_{t_s(a,b)=b_0} = \frac{\dot{\phi}_\psi(0)}{a} \tag{15}$$

on the ridge and on the intersection with the ridge, respectively. Here $\Omega(a, b)$ is the phase of the wavelet transform. It appears in practice, that the phase of the wavelet trnasform is often difficult to control in the presence of the noise in the data. Thus, Carmona *et al*. [37] proposed two improved algorithms based on the amplitude of the wavelet transform. The first one uses a concept of the parametrized ridge based on the so called "snake" functions. The second one employs the combinatorial optimization procedure. A

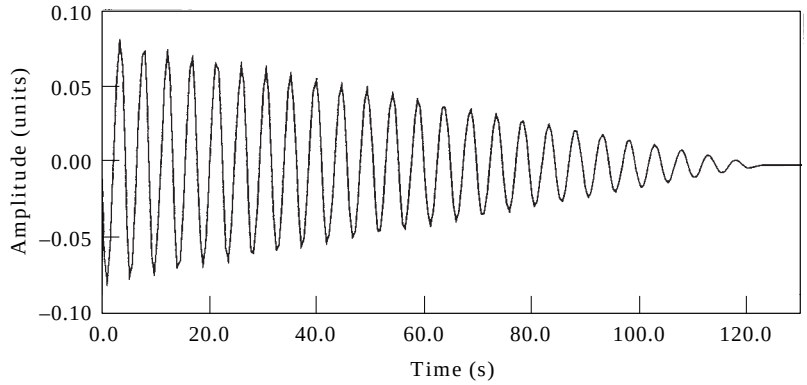

Figure 1. Impulse response function for the analyzed SDOF system.

comparative study presented in reference [37] shows that both algorithms are very effective for the ridge extraction. The simplified algorithm, based on the amplitude of the wavelet transform and involving the combinatorial optimization procedure, is used in the present work. For the sake of completeness this algorithm is described in the Appendix.

4. PARAMETER IDENTIFICATION PROCEDURE

Vibration instantaneous characteristics of restoring forces and natural frequencies can be used for system identification. In the case of non-linear systems these characteristics simply vary in time and become functions of the vibration amplitude. It has been shown in the previous section that instantaneous characteristics, namely the envelope and instantaneous frequency, can be obtained using wavelet transform ridges and skeletons. This section gives the non-linear system identification procedure based on the ridges and skeletons of the wavelet transform.

4.1. MODE DECOUPLING USING WAVELETS

The linear MDOF system is governed by the general equation,

$$[\mathbf{M}]\ddot{\mathbf{X}} + [\mathbf{C}]\dot{\mathbf{X}} + [\mathbf{K}]\mathbf{X} = \mathbf{P}, \tag{16}$$

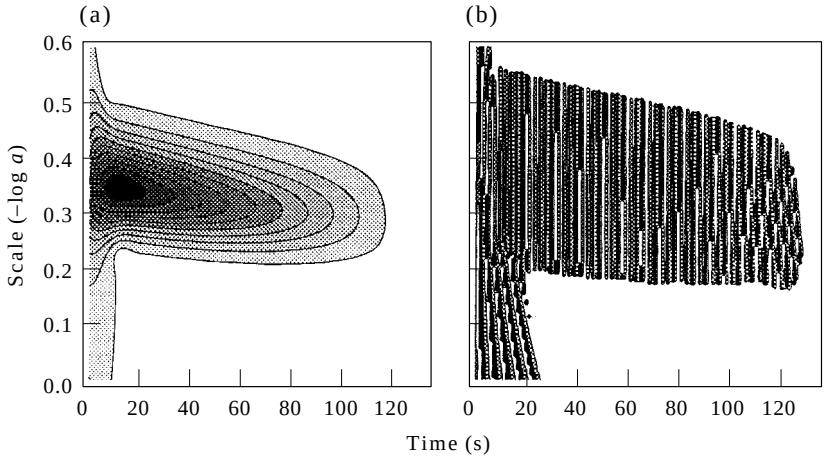

Figure 2. Wavelet transform for the impulse response function from the analyzed SDOF system: (a) amplitude; (b) phase.

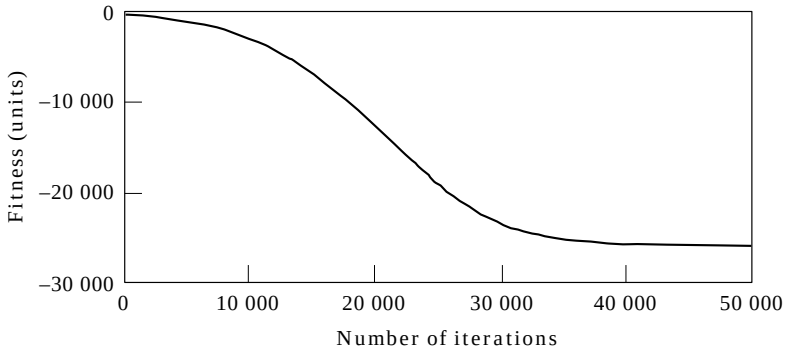

Figure 3. Graph of the fitness function for the ridge extraction procedure.

where [**M**], [**C**], [**K**] are mass, damping and stiffness matrices, respectively, and **P** is the excitation vector. The response **X** of the system can be obtained using modal analysis or a direct forced response approach. Mathematically equation (16) is in general a set of N coupled equations. If the MDOF system given by equation (16) is linear and conservative, the impulse response can be expressed by a linear combination of its modal components.

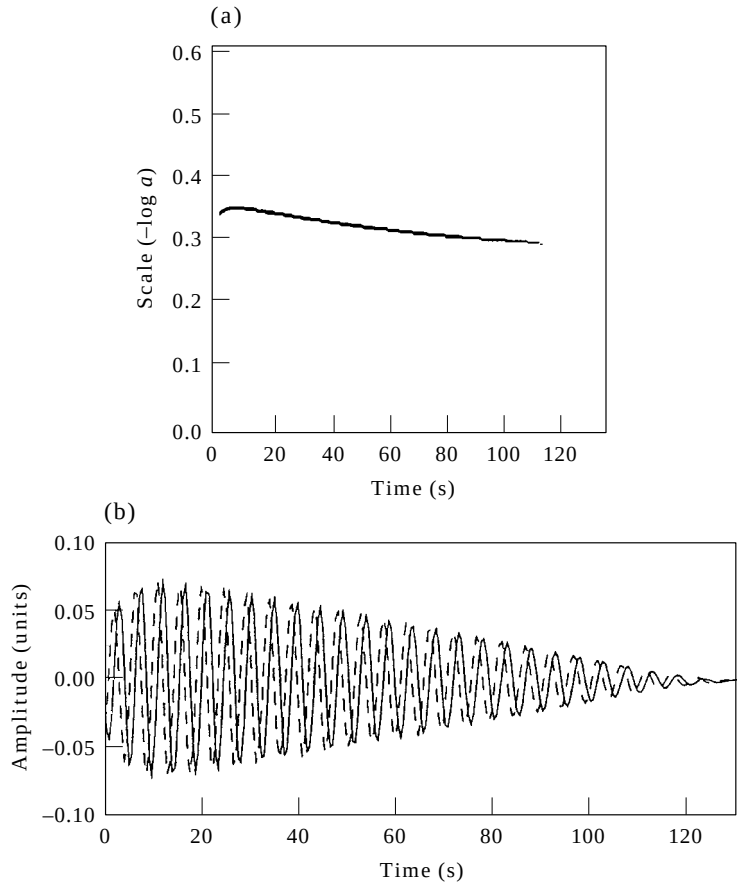

Figure 4. Ridge (a) and Skeleton (b) of the wavelet transform given in Figure 2. —, Real part; - - - , imaginary part.

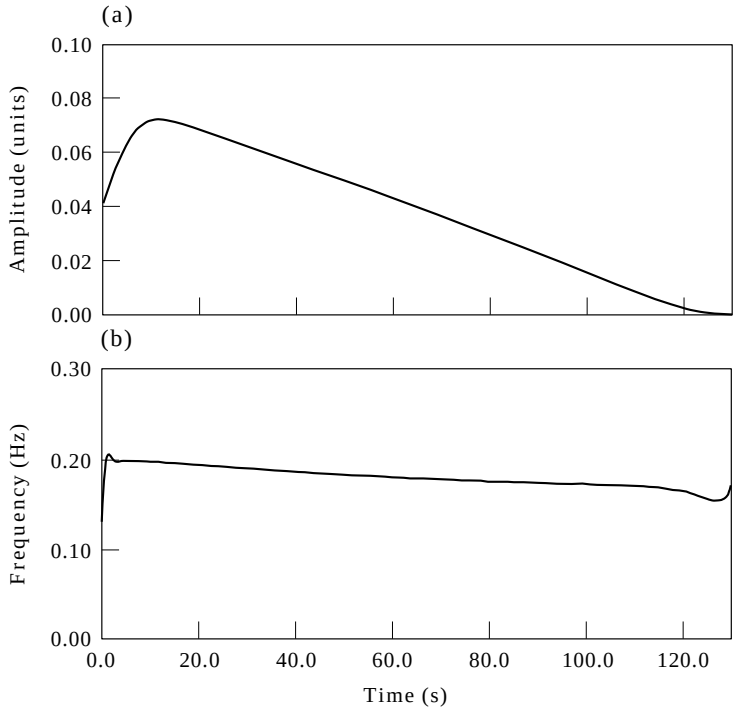

Figure 5. Instantaneous characteristics for the analyzed SDOF system: (a) envelope; (b) frequency.

In practice, when the damping is assumed to be small, N uncoupled equations similar to SDOF systems can be obtained,

$$m_i\ddot{x}_i(t) + c_i\dot{x}_i(t) + k_i x_i(t) = p_i(t), \tag{17}$$

for $i = 1, 2, \ldots, N$. The impulse response of this MDOF system can be given in general form as,

$$h(t) = \sum_{i=1}^{N} A_i \, \mathrm{e}^{-\zeta_i \omega_{n_i} t} \sin\left(\sqrt{1-\zeta_i^2}\,\omega_{n_i} t + \theta_i\right), \tag{18}$$

where ω_{n_i} is the natural frequency, N is the number of considered modes, A_i is the residue magnitude of the ith mode and ζ_i is the damping ratio. This response represents a linear combination of its single modal components. Each mode is given by an exponentially decaying harmonic function. For a non-linear MDOF system and weak non-linearities it is still possible to use the above decoupling procedure. However, it is obvious that the decay amplitude and frequency characteristics in equation (18) are no longer constant. This is discussed in section 4.2.

As shown in section 2, the wavelet transform is a signal decomposition procedure working as a filter in the time–frequency domain. Thus, it offers a possible means of uncoupling vibration modes. Since the analyzing wavelet function has compact support in the time and frequency domains, equation (3) can be re-written for multicomponent signals, using equations (5) and (7),

$$\left(W_\psi \sum_{i=1}^{N} x_i\right)(a, b) = \frac{1}{\sqrt{a}} \sum_{i=1}^{N} \int_{t - a\Delta t_\psi}^{t + a\Delta t_\psi} x_i(t) \psi^* \left(\frac{t-b}{a}\right) \mathrm{d}t. \tag{19}$$

From equations (6) and (7) this can be expressed in the frequency domain as,

$$\left(W_\psi \sum_{i=1}^{N} x_i\right)(a, b) = \sqrt{a} \sum_{i=1}^{N} \int_{f_i - \Delta f_\psi/a}^{f_i + \Delta f_\psi/a} X(f) \Psi^*_{a,b}(af)\, \mathrm{e}^{i2\pi fb}\, \mathrm{d}f. \tag{20}$$

The wavelet analyzing function for each ith mode is peaked at modal frequency f_i. For the Morlet wavelet function the relationship between frequency and dilation, and the frequency bandwidth of the filter is given by equations (8) and (9), respectively.

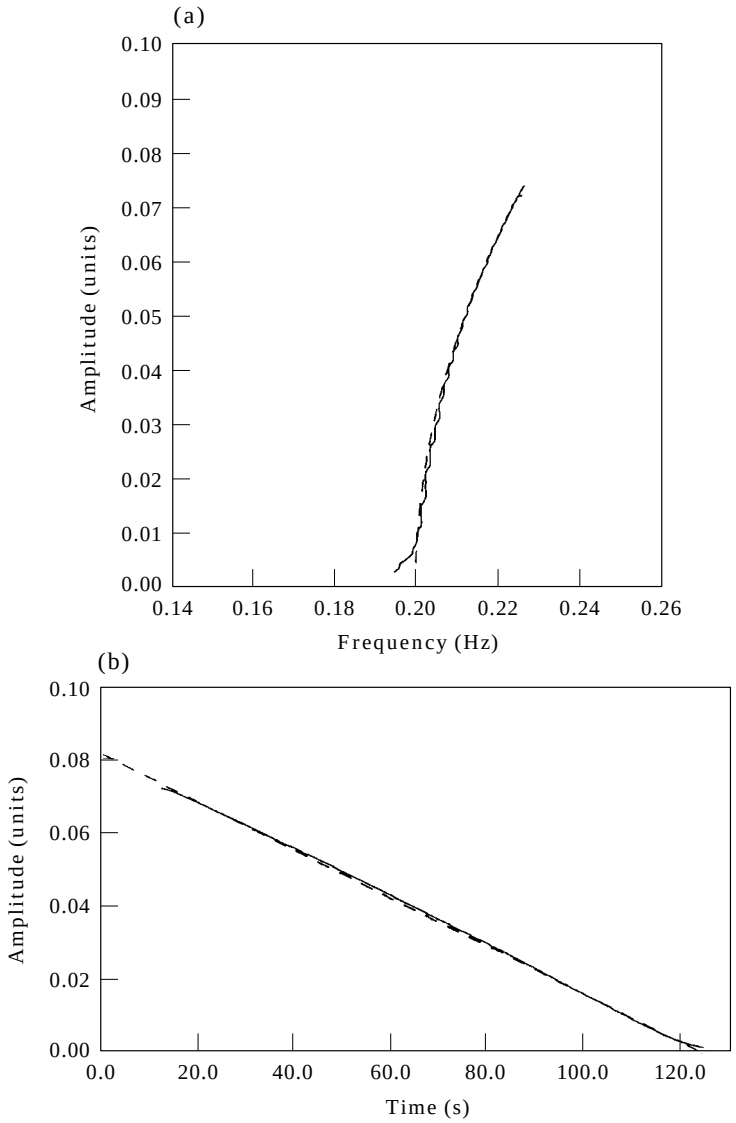

Figure 6. Backbone curve (a) and decaying envelope (b) for the analyzed SDOF system. —, wavelet analysis; - - - , theory.

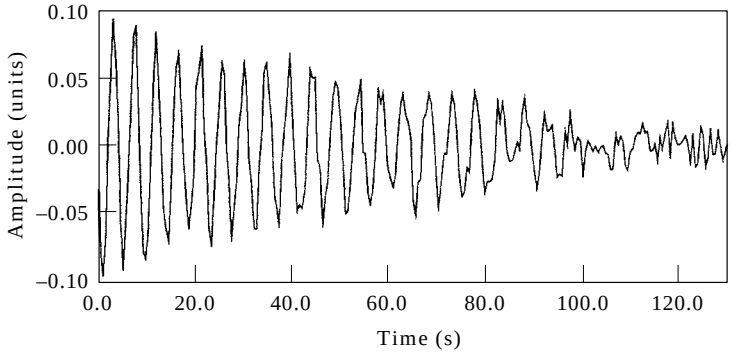

Figure 7. Impulse response function for the analyzed SDOF system in the presence of 20% noise.

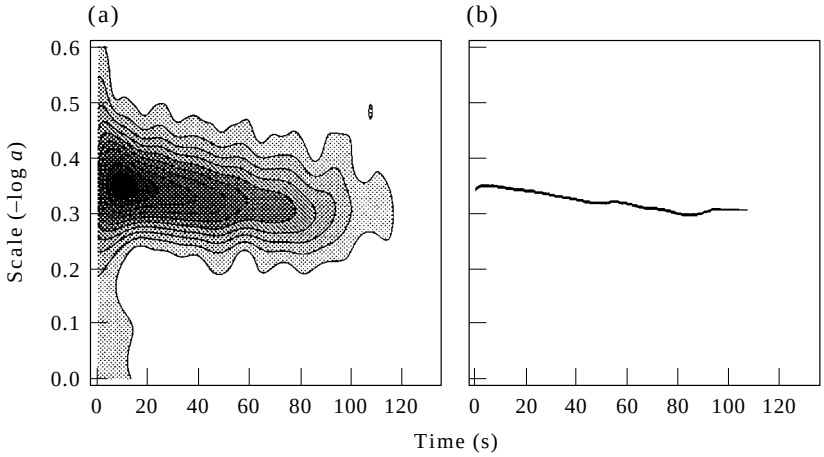

Figure 8. Wavelet transform amplitude (a) and its ridge (b) for the impulse response given in Figure 7.

4.2. NON-LINEAR BACK-BONE AND DAMPING CHARACTERISTICS

For the simple case of a linear SDOF system,

$$m\ddot{x}(t) + c\dot{x}(t) + kx(t) = p(t), \tag{21}$$

the impulse response function is given as,

$$h(t) = A_0 \, e^{-\zeta\omega_n t} \sin(\sqrt{1-\zeta^2}\omega_n t + \theta), \tag{22}$$

TABLE 1

Analyzed data sets	System identification parameters					
	Damping c	Error %	Stiffness k_1	Error %	Stiffness k_3	Error %
Theory	0·0013	–	$0{\cdot}16\pi^2 \approx 1{\cdot}558$	–	100·0	–
0% noise	0·001296	−0·3	1·586	+1·8	97·0	−3·0
5% noise	0·001320	+1·5	1·590	+2·1	96·3	−3·7
10% noise	0·001296	−0·3	1·578	+1·3	96·9	−3·1
20% noise	0·001238	−4·8	1·584	+1·7	106·7	+6·7

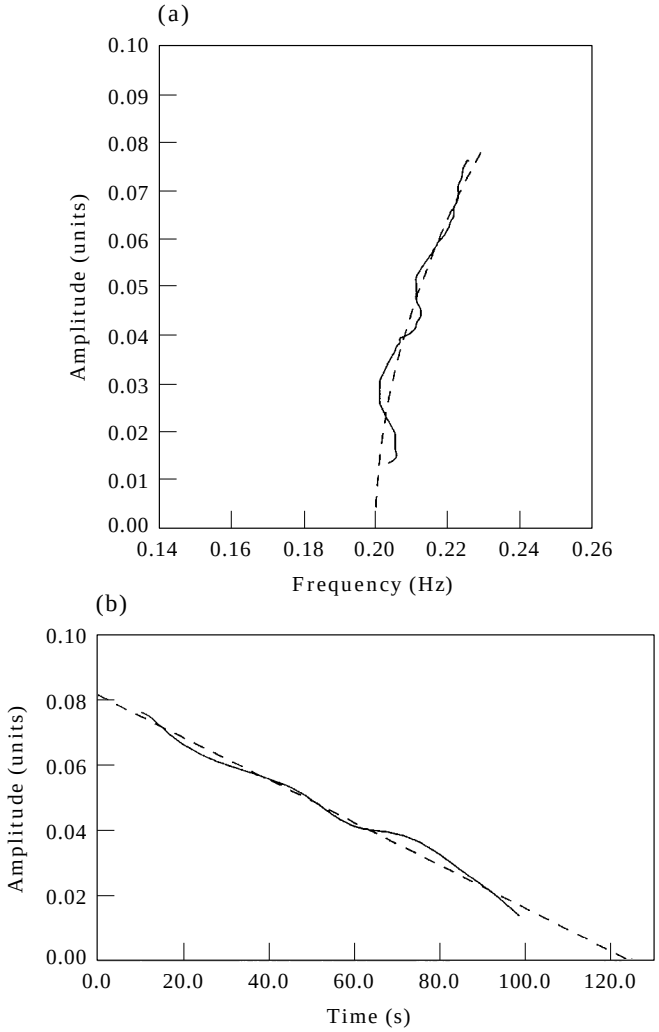

Figure 9. Backbone curve (a) and decaying envelope (b) for the analyzed SDOF system in the presence of 20% noise. —, wavelet analysis; - - - -, theory.

where ω_n is the natural frequency, A_0 is the residue magnitude and ζ is the damping ratio. Here the oscillating term is given by a sine wave at the damped natural frequency and the damping is represented by the exponentially decaying envelope. It is well known that the dissipative mechanism of the system can be detected by the analysis of the decaying envelope $A(t)$ of the impulse response function. In turn, the restoring force mechanism can be studied using the time varying frequency content $\phi(t)$ of the impulse, response function. For the system given by equation (21) the constitutive functions $A(t)$ and $\phi(t)$ are known in the explicit form as,

$$A(t) = A_0 \, \mathrm{e}^{-\zeta\omega_n t}, \qquad \phi(t) = \sqrt{1-\zeta^2}\omega_n t + \theta, \tag{23}$$

where $\zeta = c/2\sqrt{km}$, m and k are mass and stiffness of the system, respectively.

For non-linear systems the decay envelope and frequency characteristic given by equations (23) are modified according to the type of damping and stiffness non-linearities.

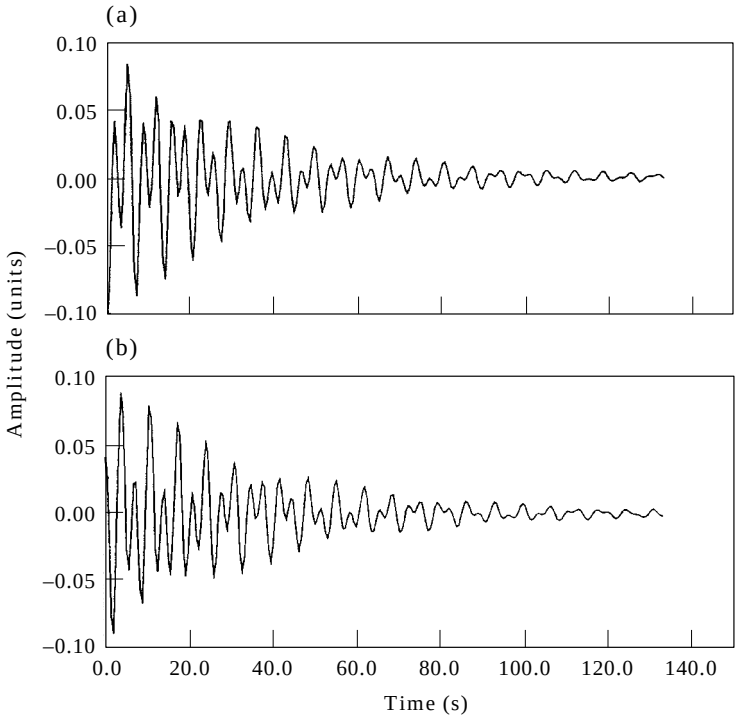

Figure 10. Impulse response functions ($x_1(t) - (a)$ and $x_2(t) - (b)$) for the analyzed MDOF system.

For simplicity, consider a non-linear SDOF system represented by the general equation of the free decay,

$$m\ddot{x}(t) + D(x, \dot{x}) = 0, \tag{24}$$

where $D(x, \dot{x})$ represents linear and non-linear damping and restoring forces. This equation can be rewritten as,

$$m\ddot{x}(t) + \omega_n^2 x + \varepsilon S(x, \dot{x}) = 0, \qquad \epsilon \ll 1, \tag{25}$$

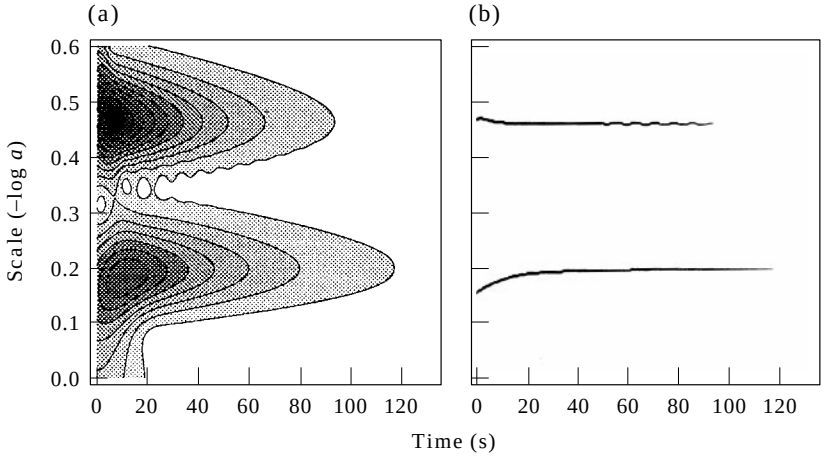

Figure 11. Wavelet transform amplitude (a) and its ridge (b) for the impulse response given in Figure 10.

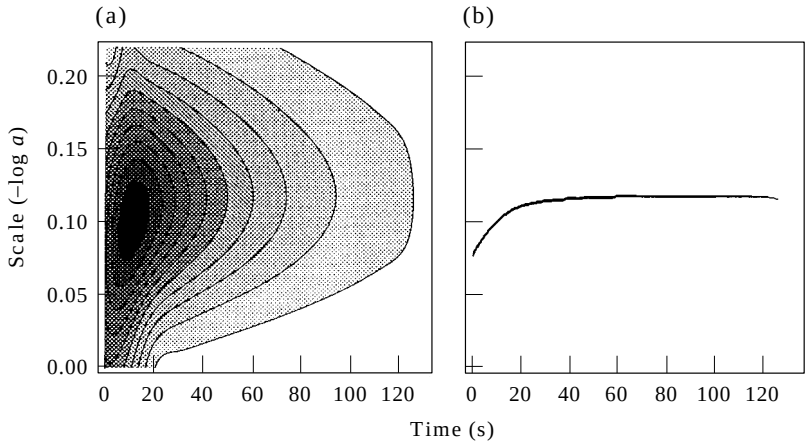

Figure 12. Wavelet transform amplitude (a) and its ridge (b) for the $x_1(t)$ impulse response function from the analyzed MDOF system.

and solved using the Kryloff–Bogoliuboff method [38]. The solution can be given in the general form of slowly-varying, time-dependent amplitude and phase functions. For a simple example of Coulomb friction, i.e., $S(x, \dot{x}) = c \operatorname{sgn}(\dot{x})$, the solution of equation (25) yields,

$$A(t) = A_0 - \frac{2c}{\pi m}\sqrt{\frac{m}{k}}\, t,$$

$$\theta(t) = \theta_0. \tag{26}$$

This clearly shows that the decay envelope for a Coulomb friction system is linear and the instantaneous frequency is constant. In contrast the linear system exhibits the exponential behaviour of the decay envelope as shown by equation (23). Other examples of instantaneous characteristics of typical non-linear systems are given in references [7, 13, 39].

Often a natural frequency and damping coefficient of a system are given as functions of the free vibration envelope A. A graphical representation of vibration behaviour in the form of a function of natural frequency versus free vibration envelope is called a backbone curve. For a linear system a backbone does not depend on the envelope and is constant. For a simple example of cubic stiffness, i.e., $S(x, \dot{x}) = kx + k_3x^3$, the backbone is given by [39],

$$f(t) = \frac{1}{2\pi}\sqrt{\frac{k}{m}}\left(1 + \frac{3}{8}\frac{k_3}{k}A^2\right), \tag{27}$$

and clearly shows the non-linear dependency of the natural frequency on the free response envelope A. Other examples can be found in references [7, 13].

The backbone and damping characteristics can be obtained from the wavelet transform ridges and then used for the system identification. Consider the solution of equation (25) in the form of the analytical signal,

$$x(t) = A(t)\, \mathrm{e}^{j\phi(t)}. \tag{28}$$

Assume that the envelope $A(t)$ is slowly varying. For the Morlet wavelet function $\psi(t)$ given by equation (4), which is also an analytic complex-valued function and has good localization properties in the frequency domain, the wavelet transform of the solution (28) can be approximated as [37],

$$(W_\psi x)(a, b) \approx A(b)\Psi^*((a\dot{\phi}(b))\, e^{j\phi(b)} + 0(|\dot{A}|, |\ddot{\phi}|), \tag{29}$$

where $\Psi^*(\cdot)$ denotes the complex conjugate of $\Psi(\cdot)$. The modulus of this function is given by,

$$|(W_\psi x)(a, b)| \approx A(b)|\Psi^*(a\dot{\phi}(b))|. \tag{30}$$

It can be seen that this modulus is maximum in the neighbourhood of the ridge defined in section 3.1. Thus, from equation (11) the instantaneous frequency of the analytical solution can be obtained from the ridge of the wavelet transform. If the ridge is known, the envelope of the signal can be approximately recovered from the skeleton of the wavelet transform following equation (30).

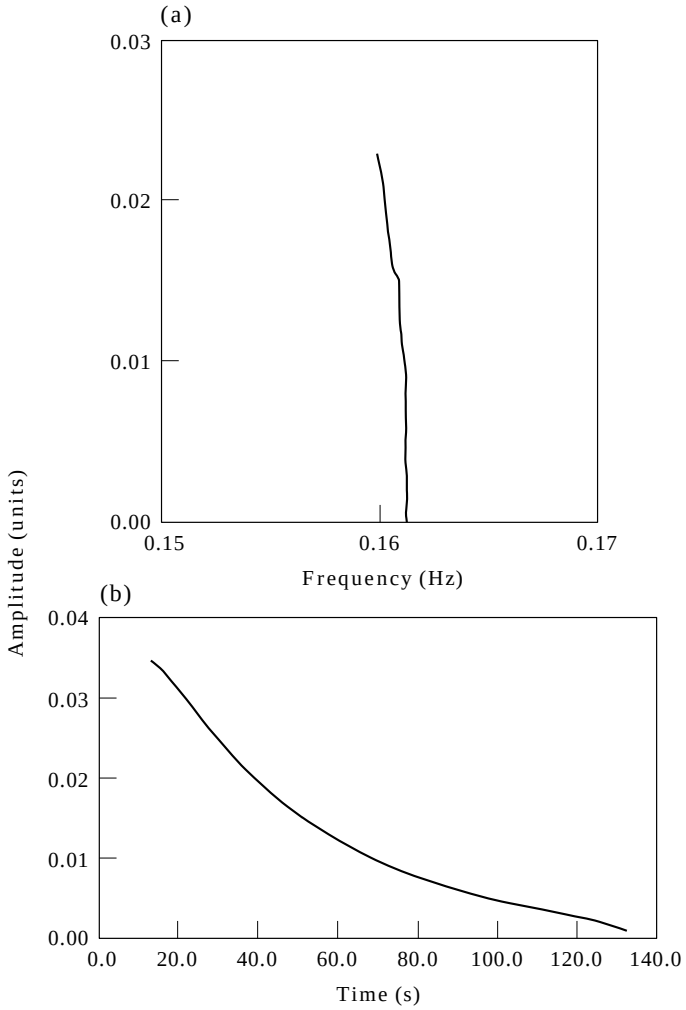

Figure 13. Backbone curve (a) and decaying envelope (b) for the first mode of the analyzed MDOF system.

The above analysis does not need to be restricted to the analytic form of the solution given by equation (28). In the case of the real valued signals, when the progressive Morlet wavelet function $\psi(t)$ is used, the corresponding wavelet transform is given by [37].

$$(W_\psi x)(a, b) = \langle x(t), \psi_{a,b}(t)\rangle = \tfrac{1}{2}\langle x_a(t), \psi_{a,b}(t)\rangle, \tag{31}$$

where $\langle x, \psi\rangle$ is the orthogonal projection of functions $x(t)$ and $\psi(t)$; $x_a(t)$ is the analytic signal of $x(t)$.

Finally, the identification procedure can be summarized in the following steps: (1) Compute the wavelet transform of the impulse response function using equation (6) and employing the classical FFT procedure. (2) Select the wavelet parameters for the mode decoupling procedure using equations (8) and (9). (3) Apply equation (20) to obtain the wavelet based mode decoupling. (4) For each mode perform the identification procedure: obtain the ridge following the algorithm given in the Appendix; compute the instantaneous frequency and envelope from the ridge of the wavelet transform using equations (11) and (30), respectively; obtain the backbone function from the instantaneous characteristics; fit the well-known decay envelope and backbone functions [39] to the characteristics obtained from the wavelet transform; obtain the values of non-linear parameters from the fitted curves.

The method of identification based on the complex envelope and Hilbert transform [7, 8] can offer a similar procedure. However, the main interest of the wavelet transform based analysis is in the context of filtering, which in the case of classical methods is performed in the time or frequency domain, and in the case of the wavelet transform analysis is realized in the combined time–scale domain. This allows one to use the method for a combination of asymptotic signals which in practice represent non-linear and time-variant behaviour of the system. Thus, the wavelet based identification procedure is more suitable for MDOF systems.

5. EXAMPLES OF IDENTIFICATION PROCEDURE

The identification procedures based on the ridges and skeletons of the wavelet transform are illustrated in this section using simulated and experimental data. The algorithms presented before were coded in C and implemented on a SUN workstation. The wavelet transform was calculated in the frequency domain as a bank of filters based on the Morlet analyzing wavelet. The details of this implementation can be found in reference [40].

5.1. SDOF SYSTEM WITH COULOMB FRICTION AND CUBIC STIFFNESS NON-LINEARITIES

The first example analyzed involves a simple SDOF system with Coulomb friction and cubic stiffness non-linearities given by,

$$m\ddot{x} + c\ \mathrm{sgn}\,(\dot{x}) + k_1 x + k_3 x^3 = 0, \tag{32}$$

where $m = 1$, $c = 0{\cdot}0013$, $k = 0{\cdot}16\pi^2$ and $k_3 = 100{\cdot}0$. The system was simulated using a fourth order Runge–Kutta procedure with non-zero initial displacement condition $x(0) = 1{\cdot}0$. The simulated impulse response is given in Figure 1(a). The simulated response was additionally corrupted by white Gaussian noise with three different levels: 5, 10 and 20% of the maximum amplitude of the data. Thus, four different sets of data were used in further analysis. Wavelet analysis was based on 512 data samples and involved the following parameters: data sampling frequency $f_s = 1{\cdot}92$ Hz, wavelet sampling frequency $f_w = 1{\cdot}68$ Hz and minimum dilation $a_{min} = 0{\cdot}25$. An example of the wavelet transform of the response is presented in Figure 2. The wavelet transform is given in the form of contour plots of its amplitude and phase. The decaying nature of the impulse response can be

observed in the amplitude of the transform. The values of the phase change from 0 to 2π. When the phase reaches 2π, it is wrapped around to the value 0. The vertical stripes represent lines of constant phase. The phase of the wavelet transform is shown here as an example and is not used in further analysis.

The amplitude based algorithm with combinatorial optimization, given in the Appendix, was applied to obtain the ridges and skeletons of the wavelet transform. Here the values of λ and μ in equation (34) were chosen to be 6×10^{-3} and 3×10^{-3}, respectively. The initial temperature C was chosen to be 3×10^{-4}. The number of iterations used was equal to 50 000. Figure 3 shows an example of the graph of the fitness function. It can be seen that the procedure reached the minimum after about 35 000 iterations. That needed about 30–40 s of computation. An example of the ridge and skeleton of the transform is given in Figure 4. Figure 5 shows the envelope and instantaneous frequency characteristics obtained from the wavelet ridge and skeleton. Small disturbances can be observed only at both ends of the instantaneous frequency. Figure 6 shows the backbone curve and decaying amplitude. Here the characteristics obtained from the wavelet transform, given by a solid line, show very good agreement with the theoretical characteristics given by a dashed line. The results clearly display cubic stiffness and dry friction non-linearities. The parameter identification procedure was performed on the basis of the backbone curve and decaying envelope. Simply the characteristics obtained from the wavelet transform were curve-fitted to the theoretical characteristics. This resulted in the values of damping and stiffness parameters equal to $c = 0{\cdot}001296$, $k_1 = 1{\cdot}586$ and $k_2 = 97{\cdot}0$. The percentage errors for these parameters are equal to 0·3, 1·8 and 3·0%. The same procedure was used to analyze the noisy data. The data was corrupted by 5, 10 and 20% of the noise. An example of the impulse response corrupted by the 20% noise is presented in Figure 7. Figure 8 shows the amplitude of the wavelet transform and the ridge obtained using the combinatorial optimization procedure. Table 1 summarizes the results of parameter identification. It can be seen that only the 20% level of noise significantly effects the values of damping (4·8% error) and non-linear stiffness (6·7% error) parameters. This results from the poor estimation of the backbone curve and decaying amplitude, as shown in Figure 9. Simply, the ridge extraction procedure, based on the wavelet amplitude and simulating annealing algorithm, gets ''trapped'' in the noise, as shown in reference [37]. In many applications, the procedure based on smoothing and subsampling can be used to improve the results [37]. However, this requires some *a priori* knowledge about the noise statistics.

It has to be mentioned that the parameter identification procedure was performed on the basis of the theoretical backbone curve and decaying envelope. The *a priori* knowledge of these characteristics was possible in the simple example studied in the paper. In general, an alternative approach could be an application of stiffness and damping forces, constructed from the instantaneous characteristics, followed by any well-known curve fitting procedure [7].

5.2. MDOF SYSTEM WITH CUBIC STIFFNESS NON-LINEARITY

For simplicity, the two-degree-of-freedom (2-DOF) system with cubic stiffness non-linearity was used as the second example. However, it is assumed that the procedure can be used for general MDOF systems. The differential equations governing the system were,

$$m_1\ddot{x}_1 + c_1\dot{x}_1 + k_1x_1 - k_3x_1^3 + k_2(x_1 - x_2) = 0, \tag{33}$$

$$m_2\ddot{x}_2 + c_2\dot{x}_2 + k_1x_2 - k_2(x_1 - x_2) = 0,$$

with $m_1 = m_2 = 1$, $c_1 = 0{\cdot}08$, $c_2 = 0{\cdot}01$, $k_1 = 1{\cdot}0$, $k_2 = 1{\cdot}2$, $k_3 = 80{\cdot}0$ and non-zero initial displacement condition $x_1(0) = 1{\cdot}0$.

The system was simulated using a fourth order Runge–Kutta procedure. Figure 10 shows the impulse responses of the system. The wavelet transform was applied to $x_1(t)$ impulse response. The analysis involved the same wavelet parameters as used previously in section 5.1. The amplitude of the wavelet transform is given in Figure 11(a). Two vibration modes can be observed. The frequencies were estimated as 0·16 Hz and 0·30 Hz. The ridge detection procedure was applied twice, separately for each mode. The simulating annealing procedure used the parameters from the previous section. The wavelet ridges can be observed in Figure 11(b). In practice the data can be decoupled before the ridge extraction procedure is performed. Since the wavelet transform is computed in the frequency domain, the decoupling procedure makes the use of equation (20) using the values of dilation obtained from equation (8) for a given value of frequency equal to 0·16 Hz. The frequency bandwidth was estimated from equation (9). Figure 12 shows the wavelet transform and its ridge for the first vibration mode. The values of wavelet sampling frequency f_w and minimum dilation a_{min} were equal to 1·4 and 0·6 Hz, respectively. More examples of wavelet based decoupling procedure, involving very close modes, can be found in reference [19]. Finally, Figure 13 shows the backbone curve and exponentially decaying amplitude for the first mode of vibration. The backbone curve in Figure 13 clearly shows the cubic stiffness non-linearity.

6. CONCLUSIONS

The method of identification of MDOF non-linear systems has been presented. The method is based on wavelet analysis of the system impulse response. The continuous wavelet transform is used for system mode decoupling. The mathematical framework of the decoupling procedure has been provided. The ridges and skeletons of the wavelet transform are used to obtain the instantaneous envelope and frequency characteristics. These characteristics are employed to obtain backbone curves and decay envelopes of the system which in turn are used for system identification. The method has been applied to simulated SDOF and MDOF systems giving satisfactory identification results. The results are not significantly effected by the presence of the noise in the data, apart from the very high level (20%) of the noise.

More studies involving simulated and experimental non-linear systems are required to fully establish the method. Further work should especially involve the analysis of MDOF systems with close modes and a comparative study with the Hilbert transform and other time–frequency based procedures.

ACKNOWLEDGMENT

It is a pleasure to express my gratitude to Dr Keith Worden at Sheffield University for his valuable comments and discussions.

REFERENCES

1. G. R. Tomlinson 1994 *Proceedings of ISMA*19—*Tools for Noise and Vibration Analysis*, *Leuwen*, *Belgium* **II**, 11–32, Linear and nonlinear—that is the question.
2. M. Feldman 1985 *Soviet Machine Science* **2**, 44–47. Investigation of the natural vibrations of machine elements using the Hilbert transform.

3. J. K. Hammond and P. Davis 1987 *Proceedings of the 5th International Modal Analysis Conference, London*. The use of enelope and instantaneous phase methods for the response of oscillatory non-linear systems to transients.
4. F. Brancaleoni, D. Spina and C. Valente 1992 In *Computational and Applied Mechanics, I—Algorithms and Theory* (C. Brezinski and U. Kulish, editors). Amsterdam: Elsevier. A free oscillation based technique for the identification of non-linear dynamic systems.
5. J. K. Lee and Y. S. Park 1992 *Proceedings of the 10th IMAC, San Diego, CA*, 167–172. Modal parameter estimation in structural system using complex envelope signal.
6. M. Feldman and S. Braun 1993 *Proceedings of the 11th IMAC*, 799–805. Analysis of typical nonlinear vibration systems by using the Hilbert transform.
7. M. Feldman 1994 *Mechanical Systems and Signal Processing* **8**, 119–127. Non-linear system vibration analysis using Hilbert Transform—I. Free vibration analysis method FREEVIB.
8. M. Feldman 1994 *Mechanical Systems and Signal Processing* **8**, 309–318. Non-linear system vibration analysis using Hilbert Transform—II. Forced vibration analysis method FORCEVIB.
9. O. Gottlieb, M. Feldman and S. C. S. Yim 1995 *Transaction of the ASME, Journal of Offshore Mechanics and Arctic Engineering* **118**, 29–36. Parameter identification of nonlinear ocean mooring systems using the Hilbert transform.
10. K. Worden 1990 *Mechanical Systems and Signal Processing* **4**, 295–319. Data processing and experiment design for the restoring force surface method, Part 1: integration and differentiation of measured time data.
11. F. Brancaleoni, D. Spina and C. Valente 1993 In *Safety Evaluation Based on Identification Approaches* (H. G. Natke, G. R. Tomlinson and J. T. P. Yao, editors). Braunschweig/ Wiesbaden: Vieweg. Damage assessment from the dynamic response of deteriorating structures.
12. M. Feldman and S. Braun 1995 *Proceedings of 13th IMAC, Nashville, TN*, 637–642. Identification of non-linear system parameters via the instantaneous frequency: application of the Hilbert transform and Wigner–Ville techniques.
13. D. Spina, C. Valente and G. R. Tomlinson 1996 *Nonlinear Dynamics* **11**, 235–254. A new procedure for detecting nonlinearity from transient data using the Gabor transform.
14. W. J. Staszewski and G. R. Tomlinson 1993 In *Safety Evaluation Based on Identification Approaches* (H. G. Natke, G. R. Tomlinson and J. T. P. Yao, editors). Braunschweig/Wiesbaden: Vieweg. Time-variant methods in machinery diagnostics.
15. W. J. Staszewski and G. R. Tomlinson 1994 In *Proceedings of ISMA19—Tools for Noise and Vibration Analysis, Leuven, Belgium*, **I**, 371–384. Fault detection procedures employing wavelet transform.
16. W. J. Staszewski and J. Giacomin 1997 In *Proceedings of the 15th IMAC, Orlando, FL*, 425–431. Application of wavelet based FRFs to the analysis of nonstationary vehicle data.
17. A. N. Robertson, K. C. Park and K. F. Alvin 1995 In *Proceedings of The Design Engineering Technical Conference, ASME-95* **DE-Vol 84.1**, 1323–1334. Extraction of impulse response data via wavelet transform for structural system identification.
18. A. N. Robertson, K. C. Park and K. F. Alvin In *Proceedings of The Design Engineering Technical Conference, ASME-95* **DE-Vol 84.1**, 1335–1344. Identification of structural dynamics models using wavelet-generated impulse response data.
19. W. J. Staszewski 1997 *Journal of Sound and Vibration* **203**, 283–305. Identification of damping in MDOF systems using time-scale decomposition.
20. W. J. Staszewski and J. E. Cooper 1996 In *Proceedings of the International Congress MV2: New Advances in Modal Synthesis of Large Structures, Non-linear, Damped and Non-deterministic Cases, Lyon, France*, 67–75. Flutter data analysis using the wavelet transform.
21. A. K. Louis 1993 In *Proceedings of the International Workshop on Inverse Problems, Hannover University, Germany*, 67–75. A wavelet approach to identification problems.
22. S. Y. Hyang, G. Z. Qi and J. C. S. Yang 1994 In *Proceedings of the 12th IMAC, Honolulu, HI*, 1162–1166. Wavelets for system identification.
23. A. N. Fedorova and M. G. Zeitlin 1997 *Preprint*. Nonlinear oscillations of a submarine via computer, Melnikov and wavelet approaches.
24. C. Surace and R. Tuotolo 1994 In *Proceedings of the 12th IMAC, Honolulu, HI*, 1141–1147. Crack detection of a beam using the wavelet transform.
25. L. Garibaldi, B. Piombo and A. Riva 1995 In 1 *Convegno Nazionale di Identificazione Structurale Centro Convegni ISMES, Seriate (BG)*. Application of wavelet transforms to dynamical system identification.

26. R. C. Micaletti, A. S. Cakmak, S. R. K. Nielsen and P. H. Kirkegaard 1996 In *Proceedings of the International Conference on Noise and Vibration Engineering ISMA*-21, *Leuven*, *Belgium*, 993–1004. Construction of time-dependent spectra using wavelet analysis for determination of global damage.
27. W. J. Staszewski 1996 In *Proceedings of the Fourth International Congress on Sound and Vibration*, *St Petersburg*, *Russia*. Nonlinear system analysis based on ridges and skeletons of the wavelet transform.
28. W. J. Staszewski and J. E. Chance 1997 In *Proceedings of the* 15*th IMAC*, *Orlando*, *FL*, 1012–1016. Identification of nonlinear systems using wavelets—experimental study.
29. I. Daubechies 1992 *Ten Lectures on Wavelets*. Philadelphia: SIAM.
30. Y. Meyer 1993 *Wavelets. Algorithms & Applications*. Philadelphia: SIAM.
31. CH. K. Chui 1992 *An Introduction to Wavelets*. In series: Wavelet Analysis and its Applications **1**: Boston, MA: Academic Press.
32. D. E. Newland 1993 *Random Vibration*, *Spectral and Wavelet Analysis*. New York: Longman, Harlow and John Wiley, third edition.
33. CH. K. Chui 1997 *Wavelets*: *A Mathematical Tool for Signal Processing*. Philadelphia: SIAM.
34. A. Grossman and J. Morlet 1985 In *Mathematics and Physics*, *Lecture on Recent Results* (L. Streit, editor). Singapore: World Scientific. Decompositions of functions into wavelets of constant shape, and related transforms.
35. W. J. Staszewski and G. R. Tomlinson 1994 *Mechanical Systems and Signal Processing* **8**, 289–307. Application of the wavelet transform to fault detection in a spur gear.
36. PH. Tchamitchian and B. Torresani 1992 In *Wavelets and their Applications* (M. B. Ruskai, editor). Boston: Jones and Bartlett Publishers. Ridge and skeleton extraction from the wavelet transform.
37. R. A. Carmona, W. L. Hwang and B. Torresani 1997 *IEEE Transactions on Signal Processing* **45**, 2586. Characterization of signals by the ridges of their wavelet transforms.
38. N. Kryloff and N. Bogoliuboff 1943 *Introduction to Nonlinear Mechanics*. Princeton, NJ: Princeton University Press.
39. A. H. Nayfeh 1978 *Perturbation Methods*. New York: John Wiley & Sons.
40. W. J. Staszewski 1994 *Ph.D. Thesis*. *Department of Engineering*, *University of Manchester*. The application of time-variant analysis to gearbox fault.
41. R. H. J. M. Otten and L. P. P. P. Ginneken 1989 *The Annealing Algorithm*. Boston, MA; Kluwer.

APPENDIX: A RIDGE EXTRACTION PROCEDURE

The algorithm of ridge extraction is briefly described below. For more details and extraction examples the reader is referred to reference [37].

The problem of ridge extraction can be considered as one of optimization. For all possible functions $a = r(b)$ over a finite set R one looks for a function which concentrates most of the energy in the time–scale domain, or in other words which follows the local maxima of the wavelet transform. This in practice leads to the optimization problem of the functional [37]

$$F(r) = -\int |(W_\psi x)(b, r_i(b)|^2 \, \mathrm{d}b + \int [\lambda \dot{r}(b) + \mu \ddot{r}(b)]^2 \, \mathrm{d}b, \tag{34}$$

where λ and μ are the parameters chosen according to the value of variance of the analyzed data. The estimate of the ridge is now the function $a = r(b)$, which minimizes the functional $F(r)$. The first term in equation (34) represents the energy of the wavelet transform restricted to the ridge. The second term in this equation is the energy of the ridge based on the local maxima representation. It is required to control the smoothness of the ridge. Carmona *et al*. [37] gives the Bayesian interpretation of the ridge extraction procedure based on the optimization scheme.

To avoid the problem of the existence of many local minima of $F(r)$ in the presence of the noise, combinatorial optimization can be used. In this paper the algorithm of simulated annealing was applied. The method is based on an analogy to thermodynamics, namely a process of annealing and the Boltzman theorem of thermal equilibrium. More details can be found in reference [41].

The simulated annealing procedure used for the minimization of $F(r)$ can be summarized in the following steps [37]:

(1) *Discretization*—represent the ridge $a = r(b)$ in the form of a finite sequence $\mathbf{r} = r(0), r(1), \ldots, r(m), \ldots, r(n-2), r(n-1)$, where $m = 0, 1, \ldots, n-1$.

(2) *Neighbourhood ridge*—define the neighbourhood ridge as a finite sequence $\mathbf{r}_n = r(0), r(1), \ldots, r(m) \mp 1, \ldots, r(n-2), r(n-1)$, where $m = 0, 1, \ldots, n-1$.

(3) *Initialization*—start the annealing procedure with the initial ridge $\mathbf{r}_0$ for a temperature $T_0 = C/\ln(2)$; compute the value of the penalty function $F(\mathbf{r}_0)$.

(4) *Step k*:

update the temperature according to $T_k = C/\ln(1+k)$;

for randomly selected integer $p \in \langle 0, n-1 \rangle$ and a number $u = \mp 1$ take the ridge $\mathbf{r}_k^c = r_k^c(0), r_k^c(1), \ldots, r_k^c(p) + u, \ldots, r_k^c(n-2), r_k^c(n-1)$;

compute the value of the penalty function $F(\mathbf{r}_k^c)$ and compare it with $F(\mathbf{r}_{k-1})$;

if $F(r_k^c) \leqslant F(r_{k-1})$ update the ridge, i.e., $\mathbf{r}_k = \mathbf{r}_k^c$;

if $F(\mathbf{r}_k^c) > F(\mathbf{r}_{k-1})$ take the random number $s (s \in \langle 0, 1 \rangle)$;

if $s \leqslant \exp - [F(\mathbf{r}_k) - F(\mathbf{r}_{k-1})]/T_k$ update the ridge, i.e., $\mathbf{r}_k = \mathbf{r}_k^c$ otherwise keep the same ridge, i.e., $\mathbf{r}_k = \mathbf{r}_{k-1}$.

This iteration procedure can be stopped after a fixed number of steps when the ridge does not change. A number of examples of ridge extraction procedure based on the phase and amplitude of the wavelet transform can be found in references [27, 28, 37].